A comparative study on near-field flow structures in a circular free jet and a square free jet

Yoshihiro Inoue[1*], Kunikazu Kondo[2] and Shintaro Yamashita[1]
[1] Department of Mechanical and Systems Engineering, Gifu University, 1-1 Yanagido, Gifu 501-1193, Japan (*Corresponding author, e-mail: inouey@gifu-u.ac.jp).
[2] Department of Mechanical Engineering, Suzuka National College of Technology, Shiroko-cho, Suzuka, Mie 510-0294, Japan

Coherent structures in the near field of a free jet have been studied. Experiments are carried out for the free jets issuing from circular and square nozzles using a water channel. Instantaneous velocity profiles are obtained in the radial directions by using an ultrasonic velocity profiler (UVP). Coherent structures in the radial direction are investigated in terms of the proper orthogonal decomposition (POD). The radial oscillation of the mixing layer is captured by the only first POD mode with about half a total energy. These velocity fields are reconstructed by the only lower-order POD modes and the reconstructed velocity fields by the lower-order and higher-order POD modes demonstrate large-scale and smaller-scale coherent structures, respectively. In the case of circular jet, there is a peak of power spectrum of the random coefficient at the first POD mode.

Keywords: Free Jet, Turbulence Intensity, Flow Structures, Proper Orthogonal Decomposition

1 INTRODUCTION

A study of the jet that is one of a representative flow field of free shear flow has been done a lot so far, and the engineering application field is wide. Investigations of turbulent jets are started for a long time, and Hinze [1] describes the prospects of those days and Rajaratnam [2] writes a monograph on turbulent jets. There are various kinds for a three-dimensional free jet from a difference of shape of an outlet. Of these, a circular jet [3], an elliptical jet [4], a rectangular jet [5-7] are well examined as a simple model.

This study is aimed for elucidation of space-time flow structure of a three-dimensional free jet by water tank experiment using an Ultrasonic Velocity Profiler (UVP). The authors have made experiments on a square and a circular jet and reported the fluctuating flow fields [8-9]. In this report, acquired data are analyzed by the proper orthogonal decomposition, and, from their results, the flow structures are compared between of the circular jet and the square jet.

2 EXPERIMENTAL PROCEDURES

2.1 Apparatus

The outline of flow field and coordinate system are shown in Fig. 1. We take *x*- and *y*-axes in the jet-axis and radial directions, respectively. Test section of the water tank used in this experiment is an open channel of 0.7 m wide, 0.64 m deep of water and 3 m long, and jet nozzle is set up at the central portion on the partition of the test section and settling chamber. The exit diameter of the circular nozzle is 85 mm, and the side length of the square nozzle is 100 mm. The contraction shape is a quadrant of a radius 12 mm added hereafter a straight line. In the experiment, Reynolds number Re_j based on the velocity U_j in the core of the jet and the equivalent diameter of nozzle D_e was set to about 1×10^4. Then the initial momentum thickness θ_0 of the shear layer at the position of x/D = 0.2 for the circular jet was about 1.0 mm, and $Re_\theta = U_j \theta_0 / \nu \approx 10^4$.

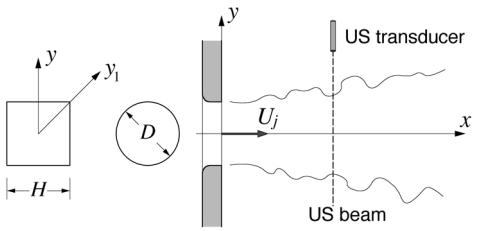

Figure 1: Coordinate system.

2.2 UVP measurement method

In the UVP measurement, ultrasonic transducer comprising a function of transmission and reception is used and velocity component in the traveling direction of ultrasonic beam is detected almost instantaneously for 128 points on the beam. The performance of the UVP measurements should be referred to Takeda [10].

The basic frequency of ultrasonic wave was 4 MHz, and hydrogen bubbles generated from a platinum wire of diameter of 0.03 mm was used for scattering particles. An incidence direction of the ultrasonic beam, namely, the measuring lines were chosen as directions of the *y*-axis and y_1-axis as shown in Fig. 1. In working conditions of this experiment, the time interval of velocity data was about 36 - 56 ms, and the space intervals of adjacent measuring point were 2.20 mm for the circular jet, and 2.90 mm for the square jet.

If a flight direction of ultrasonic beam is y, the quantity obtained by this measurement is space-time distribution of y component of the instantaneous velocity, and it is expressed with $V(y) + v(y,t)$. Here $V(y)$ shows time-averaged velocity distribution and $v(y,t)$ space-time distribution of fluctuating velocity. For data set of this space-time distribution, data analysis by the proper orthogonal decomposition is performed as done in the previous report [8], and flow structure is examined.

3 RESULTS AND DISCUSSION

3.1 Mean and fluctuating velocity distributions

In the case of both of nozzle shapes, experiments were performed at the range of $0.5 < x/D_e < 5$ in the axial direction and $-1.5 < y/D_e < 1.5$ in the lateral direction, respectively. RD is used for results of the a circular jet, and for a square jet SQ(s) is corresponding to the direction normal to the side through the jet axis and SQ(d) to the diagonal direction of the nozzle, respectively.

Figure 2 shows the distributions of mean velocity V and Fig. 3 shows the r.m.s. value of fluctuating velocity v. In the case of Fig. 2(a) for the circular jet, the distributions of mean velocity corresponding to the mixing layer formed in the initial region of for $y/D_e = 0.5$ of $x/D_e < 1$ are shown. For $x/D_e > 1.5$, the width of the flow extends outside and the peaks in their profiles move outwardly. It is shown from Fig. 3(a) that the fluctuation in the mixing layer is seen for $x/D_e > 1.5$ and the peak of the fluctuation intensity is located almost same position for the peak of the mean velocity. The peak value becomes $v_{rms}/U_j = 0.15$ and three times the value of $V/U_j = 0.05$. The fluctuation intensity on the jet-axis is augmented as goes downstream.

Distribution profile of mean velocity V_1 (Fig. 2(c)) changes in the axial direction in a similar way to RD. It is shown from the mean velocity distributions for $x/D_e < 1.5$ that width of the mixing layer is larger than RD. On the other hand, the distributions of mean velocity of SQ(s), as shown in Fig. 2(b), are different from the others. The positive mean velocity corresponding to an outward flow from the jet axis becomes about 20% of the jet velocity at $x/D_e = 1$. It is indicated that the square jet width more rapidly extends in the y-direction than in the y_1-direction. Distributions of the fluctuating intensity in the both cases of SQ(s) (Fig. 3(b)) and SQ(d) (Fig. 3(c)) become almost similar to those of RD, but the position where fluctuations start to grow up exists at more upstream position for square jet than RD.

Spatially and temporally averaged intensity of the fluctuating velocity along each measuring line is defined by the following equation,

$$E_v = \frac{1}{T}\iint v^2(y,t)\,\mathrm{d}y\,\mathrm{d}t\,. \tag{1}$$

Changes of the intensity normalized by U_j in the x-direction are shown in Fig. 4. As shown in the figure, the fluctuating energy increases gradually in the regions of $x/D_e < 3$ for RD and reaches nearly constant value in the downstream of this region. It seems that this change is caused by the distortion behavior of the vortices formed in the mixing layer, and, as shown in the previous report [8], the considerably rapid distortion of vortices are induced in $x/D_e < 1.8$ for square jets, and, as a result, the increasing of fluctuation energy is brought about.

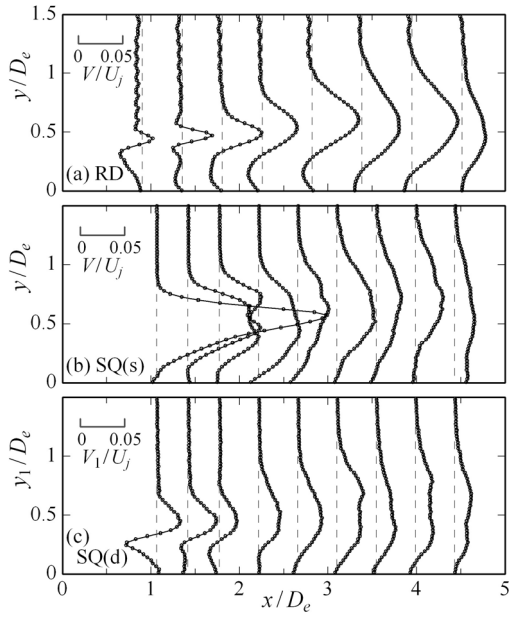

Figure 2: Distributions of the mean velocity component. (a) RD, (b) SQ(s) and (c) SQ(d)

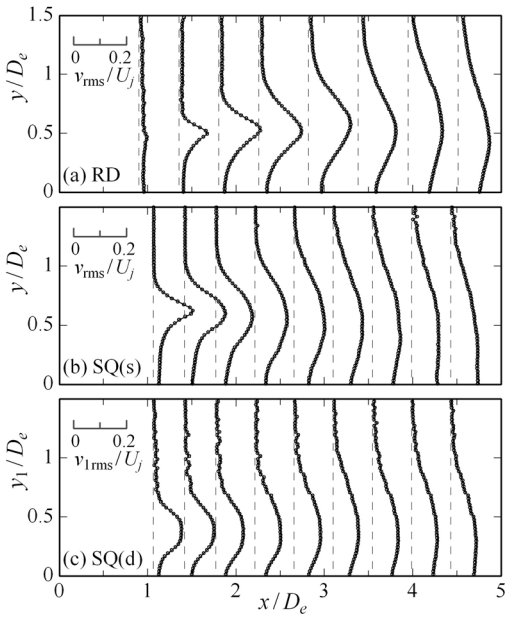

Figure 3: Distributions of the r.m.s. value of fluctuating velocity. (a) RD, (b) SQ(s) and (c) SQ(d)

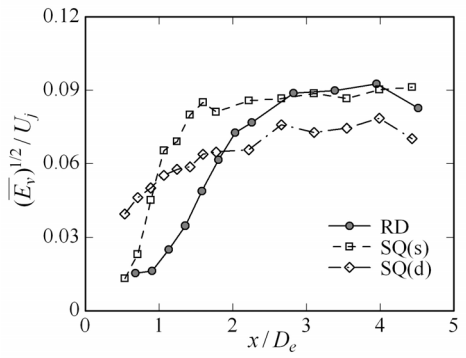

Figure 4: Change in the spatially and temporarily averaged energy of velocity fluctuation.

On the other hand, at the upstream positions, the energy for SQ(d) is most highest, however, the subsequent change of its value is slow in the downstream, and the value don't reach the level of others at x/D_e = 5. The averaged energy of velocity fluctuation for SQ(s) rapidly increases and becomes nearly constant for x/D_e > 1.5.

3.2 Flow structures

The proper orthogonal decomposition (POD) [11-13] is a method that is expanded empirically and efficiently the fluctuating flow fields in space to any modes, and its details were mentioned in the previous report [8].

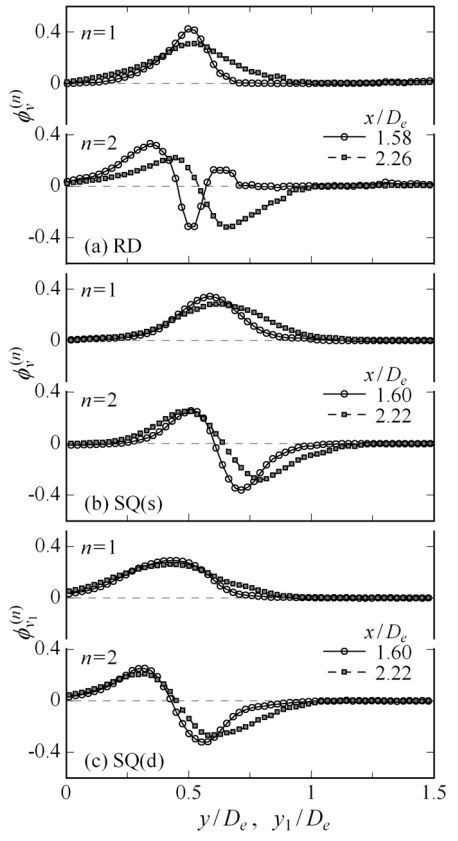

Figure 5: Distributions of the eigenfunction at the first two POD modes. (a) RD, (b) SQ(s) and (c) SQ(d)

Figure 5 shows the distributions of the eigenfunction for n = 1 and 2. There is no conspicuous characteristic of the eigenfunction for all the velocity distributions of RD, SQ(s) and SQ(d). The eigenfunction at first mode indicates fundamental oscillation in transverse direction, and the eigenfunction at second mode indicates its higher-order components. It seems that only second mode at x/D_e = 1.58 for RD has a different distribution from the others, however, this shape is similar to the third mode of the others.

The eigenvalue $\lambda^{(n)}$, namely, stock energy at each mode is satisfied following relation,

$$E_v = \sum_n \lambda^{(n)} . \tag{2}$$

Figure 6 shows the changes in the axial direction of energy contribution rate from n = 1, n = 1 to 3 and n = 1 to 5 to total fluctuating energy. The sum of n = 1 to 5 include nearly 80% of energy in any modes, and hence this flow field can be well expressed by the relatively lower-order POD mode only. For n = 1, its energy content decreases as goes downstream from a peak of nearly 60 %, the energy included n = 2 to 3 relatively increase.

Random coefficients of the fluctuating velocity distributions $v(y,t)$ is defined by the following equation,

$$v^{(n)}(t) = \int v(y,t)\,\phi^{(n)}(y)\,\mathrm{d}y , \tag{3}$$

and indicates the change in time of the contribution of spatial mode.

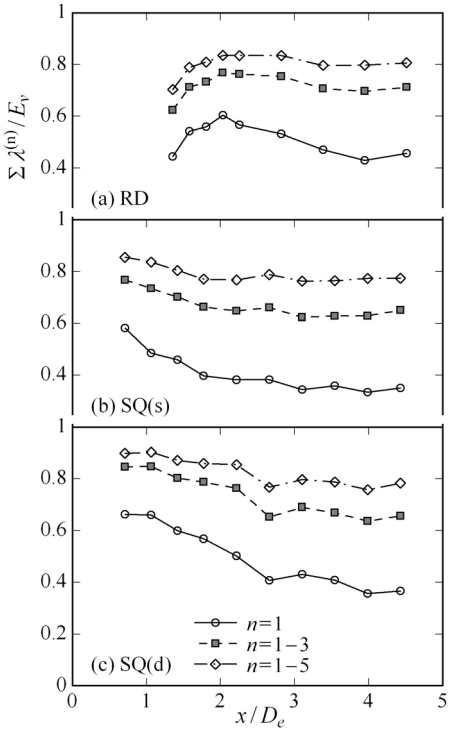

Figure 6: Contributions from several POD modes to the total fluctuating energy. (a) RD, (b) SQ(s) and (c) SQ(d)

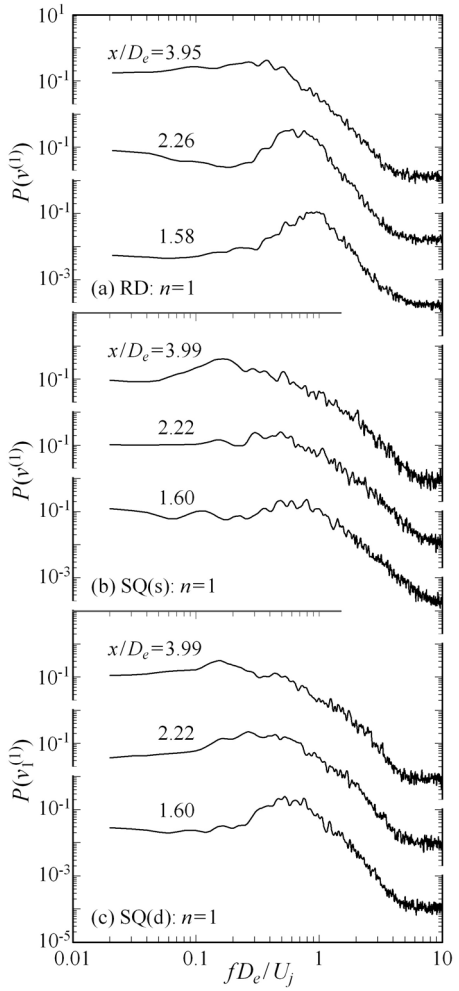

Figure 7: Power spectra of the random coefficient at the first mode. (a) RD, (b) SQ(s) and (c) SQ(d)

The power spectrum obtained from the FFT analysis of random coefficient for n = 1 on the three whole cross sections in each direction is shown in Fig.7. From this spectrum, the time periodicity of the spatial variation of mode n = 1 can be examined. For RD there exists a clear hill on the distributions of spectra for x/D_e = 1.58 and 2.26, and mean frequency is $f\ D_e/U_j$ = 0.94 at x/D_e = 1.58, and this value decreases as goes downstream. On the other hand, the spectrum width for SQ(s) becomes considerably broad, and the spectrum width for SQ(s) is narrow compared with that for SQ(s).

4 CONCLUSIONS

About velocity distributions in the radial direction for circle and square free jet, the fluctuating energy increase in the axial directions in any flow fields, and the value approaches value around 0.09, but the tendency to increase is different respectively, and the increase stopped at nearly x/D_e = 2. Also, there was no essential difference of the distribution of each eigenfunction, and any difference between energy contribution rates from lower-order POD mode in space was hardly seen. That is to say, it is enable to compare the characteristics in time of the flow with the random coefficients that indicates the time contribution of from spatial modes. When this power spectrum was investigated, the different distributions were obtained in each case for x/D_e < 3.

REFERENCES

[1] Hinze JO: Turbulence, An Introduction to its Mechanism and Theory, McGraw-Hill, New York (1959).
[2] Rajaratnam N: Turbulent Jets, Elsevier Sci. Pub., Amsterdam (1976).
[3] Wygnanski I, Fiedler H: Some Measurements in the Self-preserving Jet, J. Fluid Mech. 38 (1969) 577-612.
[4] Husain HS, Hussain F: Elliptic Jets. Part 3. Dynamics of Preferred Mode Coherent Structure, J. Fluid Mech. 248 (1993) 315-361.
[5] Tsuchiya Y, Horikoshi C, Sato T: On the Spread of Rectangular Jets, Exp. Fluids 4 (1986) 197-204.
[6] Toyoda K, Hiramoto R: Vortical Structure and Diffusion Mechanism of a Rectangular Jet, Proc. 3rd ASME/JSME Joint Fluids Eng. Conf., San Francisco, USA (1999) FEDSM99-6946.
[7] Gutmark E, Grinstein FF: Flow Control with Noncircular Jets, Annual Rev. Fluid Mech. 31 (1999) 239-272,
[8] Inoue Y, Yamashita S, Kondo K: The Ultrasonic Velocity Profile Measurement of Flow Structure in the Near Field of a Square Free Jet, Exp. Fluids 32 (2002) 170-178.
[9] Inoue Y, Yamashita S, Kondo K: Experiments in an Initial Region of a Circular Free Jet, Proc. 4th ISUD, Sapporo, Japan (1999).
[10] Takeda Y: Velocity Profile Measurement by Ultrasonic Doppler Method, Exp. Thermal Fluid Sci. 10 (1995) 444-453.
[11] Arndt REA, Long DF, Glauser MN: The Proper Orthogonal Decomposition of Pressure Fluctuations Surrounding a Turbulent Jet, J. Fluid Mech. 340 (1997) 1-33.
[12] Berkooz G, Holmes P, Lumley JL: The Proper Orthogonal Decomposition in the Analysis of Turbulent Flows, Annual Rev. Fluid Mech. 25 (1993) 539-575.
[13] Sirovich L, Kirby M, Winter M: An Eigenfunction Approach to Large Scale Transitional Structures in Jet Flow, Phys. Fluids A2 (1990) 127-136.